

# SiAlON ceramics from nanopowders

Ilmars Zalite<sup>a,\*</sup>, Natalja Zilinska<sup>a</sup>, Gottfried Kladler<sup>b</sup>

<sup>a</sup> Institute of Inorganic Chemistry of the Riga Technical University, 34 Miera Str., Salaspils LV-2169, Latvia

<sup>b</sup> ARC Seibersdorf Research GmbH, A-2444 Seibersdorf, Austria

Available online 22 October 2007

## Abstract

Different compositions of  $\alpha$ - and  $\alpha$ -/ $\beta$ -SiAlON materials have been prepared from two different starting powders (commercial and nanopowder). Separate nanopowders and their composites were used as nanocomponents:  $\text{Si}_3\text{N}_4$ , 90% $\text{Si}_3\text{N}_4$ –10%AlN, 90%AlN–10% $\text{Y}_2\text{O}_3$ ,  $\text{Si}_3\text{N}_4$ –AlN– $\text{Al}_2\text{O}_3$ – $\text{Y}_2\text{O}_3$  and  $\text{Y}_2\text{O}_3$ , produced by the method of plasma-chemical synthesis. Powder mixtures of the same composition from  $\alpha$ - $\text{Si}_3\text{N}_4$  powder (Ube grade SN-E10) and additives ( $\text{Y}_2\text{O}_3$ ,  $\text{Al}_2\text{O}_3$  and AlN) produced by a conventional powder mixture process were used for comparing. Compositions have been pressure less sintered under nitrogen atmosphere until 1650 °C with a heating rate of 10 °C/min and holding time of 2 h. The densification behavior of the materials depends on the powder composition and the size of the particles used for starting powder. It is possible to obtain dense materials from nano-sized powder at relatively low temperatures (1500–1600 °C) with good mechanical room temperature properties in comparison with material made of a  $\mu\text{m}$ -sized starting powder.

© 2007 Elsevier Ltd. All rights reserved.

**Keywords:** SiAlON; Nanocomposites; Sintering; Grain size; Mechanical properties

## 1. Introduction

Majority of  $\text{Si}_3\text{N}_4$  based ceramics (e.g. SiAlON) are made from powders and therefore depend to a large extent on the quality of the starting powders. The diffusion velocity and the length of diffusion way are of great importance for compacting of covalent compounds, for example  $\text{Si}_3\text{N}_4$  and SiAlONs. The length of diffusion way can be decreased by using nanocomponents for production of compact material. As it is obvious from many investigations of compacting, the application of  $\text{Si}_3\text{N}_4$  nanopowders makes possible to decrease the sintering temperature and to accelerate the sintering process<sup>1</sup> resulting in material with more fine-grained structure<sup>2</sup> and modified properties<sup>3</sup>.

Results on preparation of SiAlON ( $\alpha$ -,  $\alpha$ -/ $\beta$ -) materials of differing compositions from nanocomponents by sintering in nitrogen atmosphere until 1650 °C are summarised in this work and these results are compared with results obtained from commercial  $\mu\text{m}$ -sized starting powders.

## 2. Experimental

SiAlON materials were prepared by application of both mixtures of separate nanopowders, and nanopowder composites obtained by nanopowder synthesis. These nanopowders were prepared via plasma-chemical synthesis in nitrogen plasma, using metallic (Si, Al) and oxide ( $\text{Y}_2\text{O}_3$ ,  $\text{Al}_2\text{O}_3$ ) powders as raw materials.<sup>4</sup> Five plasma-synthesized nanopowders were used— $\text{Si}_3\text{N}_4$ , the mixture of 90% $\text{Si}_3\text{N}_4$ –10%AlN, 90%AlN–10% $\text{Y}_2\text{O}_3$ ,  $\text{Si}_3\text{N}_4$ –AlN– $\text{Al}_2\text{O}_3$ – $\text{Y}_2\text{O}_3$  and  $\text{Y}_2\text{O}_3$ . Their characteristics are given at Table 1. The  $\text{Si}_3\text{N}_4$  nanopowder contains up to 50% of crystalline  $\text{Si}_3\text{N}_4$  (ratio  $\alpha$ -/ $\beta$ - is approximately 1:1), the rest is amorphous phase of  $\text{Si}_3\text{N}_4$ . Micrographs of some nanopowders are given in Fig. 1.

Composition of investigated  $\alpha$ - and  $\alpha$ -/ $\beta$ -SiAlON composites is represented in a phase diagram<sup>5</sup>  $\text{Si}_{12}\text{N}_{16}$ – $\text{Al}_{12}\text{O}_{12}\text{N}_4$ – $\text{Y}_4\text{Al}_{12}\text{N}_{16}$  (Fig. 2) and is given in Table 2.

The specimens 1–5 lie on the line  $\text{Si}_3\text{N}_4$ –(9AlN·1 $\text{Y}_2\text{O}_3$ ) and were made from mixture of  $\text{Si}_3\text{N}_4$  and 9AlN–1 $\text{Y}_2\text{O}_3$  nanopowders. Specimen 3 was obtained also by using  $\text{Si}_3\text{N}_4$ –AlN and  $\text{Y}_2\text{O}_3$  nanopowders (sample No. 3\*). Samples 6 to 10 are of higher oxygen content and are situated away from the line  $\text{Si}_3\text{N}_4$ –(9AlN·1 $\text{Y}_2\text{O}_3$ ). They were made by using  $\text{Si}_3\text{N}_4$ –AlN (samples 6–8) and  $\text{Si}_3\text{N}_4$ –AlN– $\text{Al}_2\text{O}_3$ – $\text{Y}_2\text{O}_3$  (samples 9 and 10) nanocomposites and small amount of AlN (H.C. Starck,

\* Corresponding author.

E-mail address: [ilmars@nki.lv](mailto:ilmars@nki.lv) (I. Zalite).

Table 1  
Chemical composition and size distribution of the starting powders

Powder	Chemical composition (wt.%)					BET (m <sup>2</sup> /g)	d <sub>50</sub> (nm)
	Si <sub>3</sub> N <sub>4</sub>	AlN	Al <sub>2</sub> O <sub>3</sub>	Y <sub>2</sub> O <sub>3</sub>	Si <sub>free</sub>		
Si <sub>3</sub> N <sub>4</sub>	98.1	–	–	–	0.7	55	40
Y <sub>2</sub> O <sub>3</sub> –AlN	–	89.1	–	9.8	–	30	60
Si <sub>3</sub> N <sub>4</sub> –AlN	85.8	9.7	–	–	0.6	50	40
Si <sub>3</sub> N <sub>4</sub> –AlN–Al <sub>2</sub> O <sub>3</sub> –Y <sub>2</sub> O <sub>3</sub>	83.7	8.0	2.6	4.1	1.3	70	30
Y <sub>2</sub> O <sub>3</sub>	–	–	–	100	–	25	65

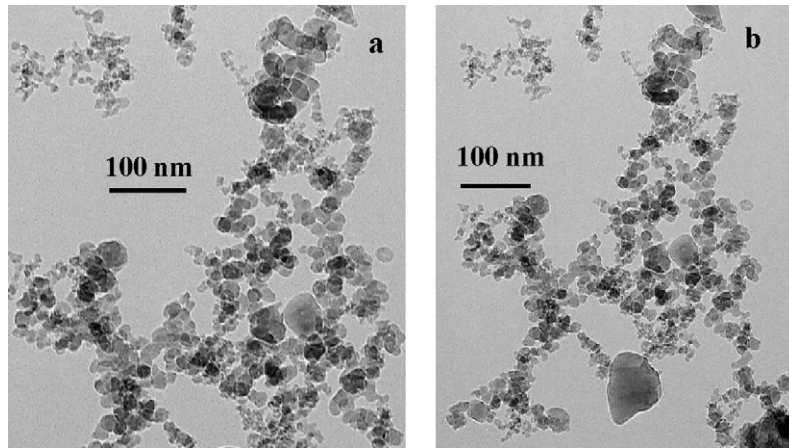


Fig. 1. Micrographs of Si<sub>3</sub>N<sub>4</sub>–AlN (a) and Si<sub>3</sub>N<sub>4</sub>–AlN–Al<sub>2</sub>O<sub>3</sub>–Y<sub>2</sub>O<sub>3</sub> (b) nanoparticles.

grade B), Y<sub>2</sub>O<sub>3</sub> (H.C. Starck, grade C) and Al<sub>2</sub>O<sub>3</sub> (Alcoa Chemie GmbH, A16SG) powder additions for correcting of the composition. Simultaneously the SiAlON powders of the same composition were prepared from commercial powders (marked from 1C to 10C). The starting material for the conventionally prepared SiAlON consists of a mixture of α-Si<sub>3</sub>N<sub>4</sub> (UBE, SN-10E), AlN (H.C. Starck Grade C), Al<sub>2</sub>O<sub>3</sub> (Alcoa Chemie GmbH, A16SG) and Y<sub>2</sub>O<sub>3</sub> (Nanophase) powders.

All powders were mixed with 2 wt.% of stearic acid, homogenized in hexane for 15 h in a rotating polyethylene bottle with silicon nitride balls, and afterwards treated for 2 h in ultrasonic

Table 2  
Composition of specimen (wt.%)

No.	Si <sub>3</sub> N <sub>4</sub>	AlN	Al <sub>2</sub> O <sub>3</sub>	Y <sub>2</sub> O <sub>3</sub>	Phase range (theoretic)
1	70.2	18.5	–	11.3	α'
2	76.5	14.6	–	8.9	α'
3	82.5	10.8	–	6.7	α' + β'
4	90.4	6.0	–	3.6	α' + β'
5	95.5	2.8	–	1.7	α' + β'
6	68.6	16.4	2.8	12.2	α'
7	73.4	15.5	3.2	7.9	α'
8	81.6	9.4	3.3	5.7	α'
9	72.8	16.9	2.2	8.1	α'
10	85.8	7.3	2.7	4.2	α' + β'

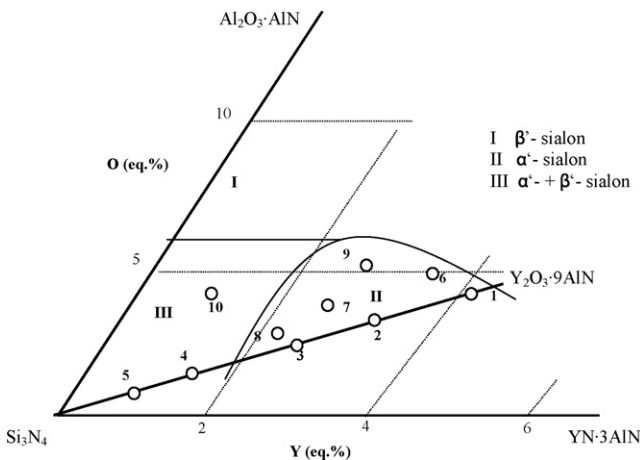


Fig. 2. Specimen composition spots in the phase diagram of the Y–Si–Al–O–N system.

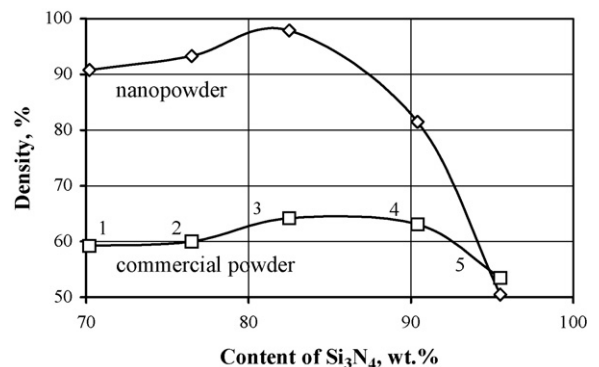


Fig. 3. Density of samples 1–5 sintered at 1650 °C depending on composition.

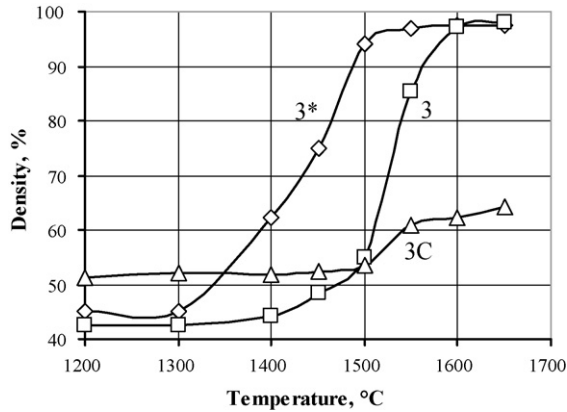


Fig. 4. Changes of the relative density during sintering of specimen 3.

bath. After drying at 80 °C the powders were sieved through a 200  $\mu\text{m}$  mesh. Green bodies with a diameter of 15 mm and a height of 7–8 mm were produced by die pressing with a pressure of 200 MPa. The densities of samples (“green body”) pressed from nanopowders were 40–48% and from conventional powders about 50–57%.

After removing of the stearic acid at 600 °C the samples were pressure-less sintered under nitrogen atmosphere up to 1650 °C with a heating rate of 10 °C/min, and holding time for 2 h.

The chemical composition of the nanopowders (N, Si<sub>free</sub>, Y, Al) was determined by the chemical analysis. Phase com-

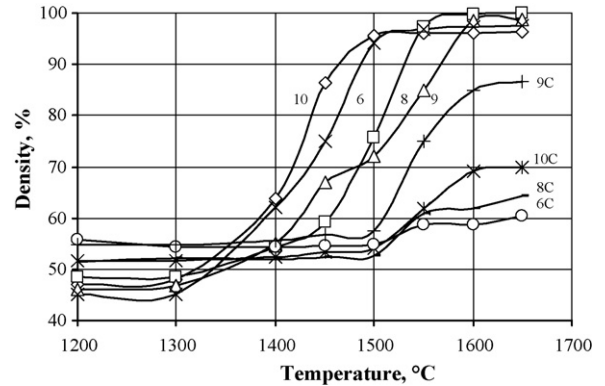


Fig. 5. Changes of the relative density during sintering of all specimens.

position of the sintered specimens was performed via X-ray diffractometry (XRD). The size and morphology of particles were determined by the transmission electron microscopy (TEM). The microstructure was observed using scanning electron microscopy (SEM) on fracture surfaces. Density of the sintered samples was determined by the Archimedes method. Hardness (loads: 98 and 49 N) and fracture toughness (load: 98 N) were measured by the Vickers indentation technique.

### 3. Results and discussion

The sinterability depends on composition in cross-section  $\text{Si}_3\text{N}_4\text{-9AlN}\cdot\text{1Y}_2\text{O}_3$ : for samples from 1 to 3 this increases,

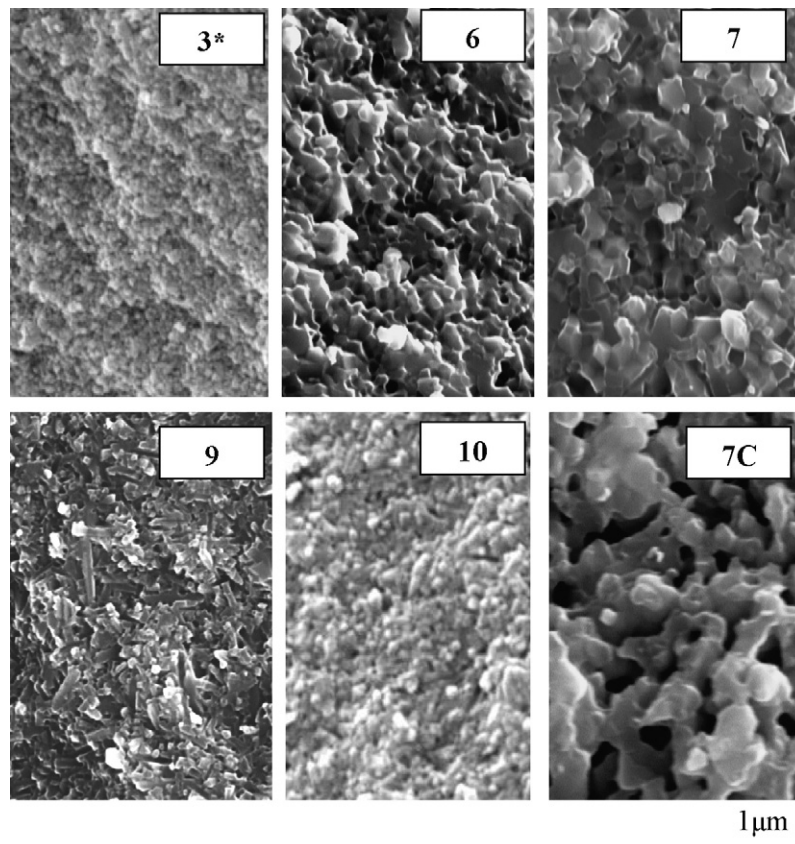


Fig. 6. Microstructure of samples sintered at 1650 °C.

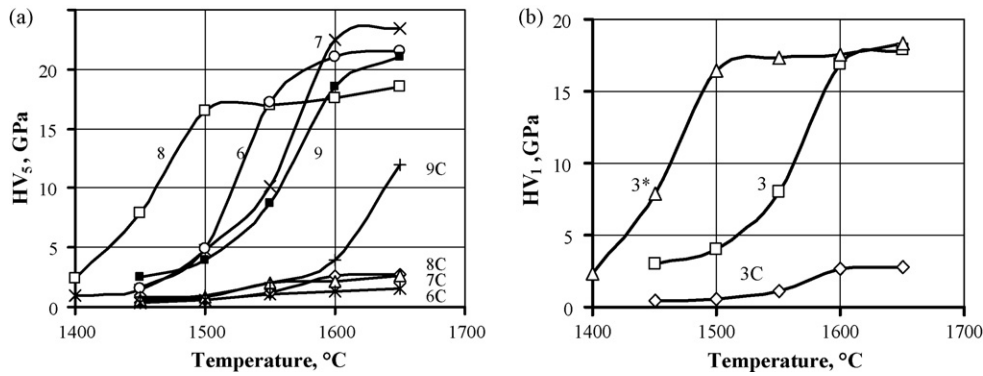


Fig. 7. Hardness of SiAlON samples 6–9 (a) and 3 (b) depending on sintering temperature.

but rapidly decreases when the amount of sintering additives decreases (samples 4 and 5) (Fig. 3). Samples 2 and 3 reach maximum density. Sample 3 has maximum density already at 1600 °C, but sample 3\* sinters at more low temperature of 1500–1550 °C (Fig. 4).

Sintering of  $\alpha$ -SiAlONs of other composition and sintering of  $\alpha/\beta$ -SiAlONs takes place as much as fast and at the same temperatures (until 1600 °C) as in the case of samples 2 and 3 (Fig. 5).

It is obvious that samples from nanopowders sinter more easily and at more low temperatures in comparison with SiAlONs of the same composition from industrial powders. The commercial powders almost do not sinter at temperatures up to 1650 °C—the change of density is from 50–54% (“green body”) to 60–70% at the temperature of 1650 °C. Sample 9C reached the maximum density of 87%.

The phase formation differs in the case of sintering of commercial and nanopowders. While in the case of commercial powders  $\alpha$ -SiAlON forms directly from  $\alpha$ -Si<sub>3</sub>N<sub>4</sub> already at 1450 °C, the transformation of  $\alpha$ -Si<sub>3</sub>N<sub>4</sub> to  $\alpha$ -SiAlON was not completely finished at 1650 °C. In the case of nanopowders the amorphous Si<sub>3</sub>N<sub>4</sub> firstly crystallizes into the  $\alpha$ - and  $\beta$ -Si<sub>3</sub>N<sub>4</sub> until 1400 °C, but above 1400–1450 °C  $\beta$ -SiAlON begins to form. At temperatures 1500–1550 °C also  $\alpha$ -SiAlON forms and its amount increases with the increase of temperature. The phase composition of samples sintered at 1650 °C depends on the starting chemical composition and contains either mainly  $\beta$ -SiAlON (10),<sup>6</sup> or mixed  $\alpha$ - and  $\beta$ -SiAlONs (7, 8, 9), or only  $\alpha$ -SiAlON (6). As it is obvious, the temperature of 1650 °C is too low for formation of  $\alpha$ - or  $\alpha/\beta$ -SiAlON phases corresponding with the phase diagram.

The microstructure of samples depends on their chemical composition. The crystallite size of samples (both for  $\alpha$ - and  $\beta$ -SiAlON phases) obtained from nanopowders at 1650 °C is  $\sim$ 100 nm. The grain size of samples prepared from nanopowders at temperatures up to 1600 °C changes insignificantly and is in the range of 200–300 nm. Also at the temperature of 1650 °C the grain size of sintered samples does not change noticeably, except sample 7, where the grain size increases a little bit (Fig. 6). Significant formation of needle-shaped crystals (samples 8, 10 and especially 9) begins at the temperatures of 1600–1650 °C. The average size of needle-shaped crystals

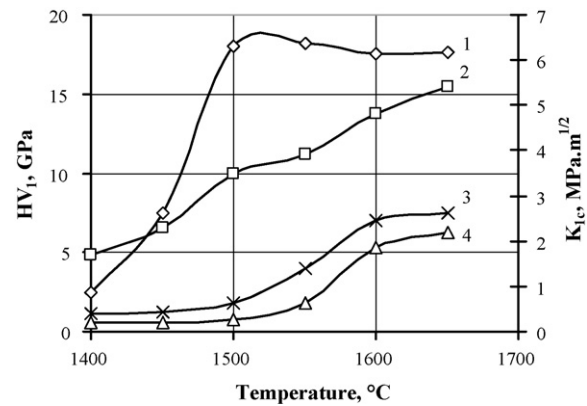


Fig. 8. Changes of material properties—hardness (1, 4) and fracture toughness (2, 3) during the sintering process. 1, 2—sample 10; 3, 4—sample 10C.

is about 200 nm in diameter and up to 2  $\mu$ m in length. The microstructure of samples sintered at 1650 °C from commercial powders is porous and the grain size is in the range of 0.5–1.0  $\mu$ m.

The hardness of sintered materials is directly related to their density, as it is shown in Fig. 7a. The Vickers hardness of the samples prepared from nanopowders was in a range of HV<sub>5</sub> = 18–23 GPa. The highest hardness was observed for sample 7, which has the least needle-shaped crystals. The Vickers hardness of the nanopowder samples 3 and 3\* was determined in a range of HV<sub>1</sub> = 18–19 GPa (Fig. 7b).

Materials from industrial powders are not fully sintered, therefore their hardness is small (HV<sub>5</sub> = 2–3 GPa). Only the sample 9 is more dense and with higher hardness.

Also the hardness of two-phase ( $\alpha$ - +  $\beta$ -SiAlON) samples is changing proportionally to the density, and the sample (10) from nanopowder reaches the maximum hardness (HV<sub>1</sub> = 17.5–19 GPa) already after sintering at temperatures of 1500–1550 °C (Fig. 8). The fracture toughness increases with the increase of sintering temperature and developing microstructure, including the growth of needle-shaped crystals.

#### 4. Conclusions

The results of this study show that the densification behavior of the SiAlON materials depends on the powder composi-

tion and the size of the particles used as starting powder. The samples with the composition at the area of  $\alpha$ -SiAlONs sinter more easily. It is possible to obtain dense materials from nano-sized powder at relatively low temperatures (1500–1600 °C) with good mechanical room temperature properties in comparison with material made of a  $\mu\text{m}$ -sized starting powder. Exception is the sample from  $\text{Si}_3\text{N}_4$ -AlN and  $\text{Y}_2\text{O}_3$  nanopowders—this begins to sinter intensively already at 1300 °C and reaches the maximum density already at 1500 °C.

The grain size of SiAlON materials prepared from nanopowders is smaller (200–300 nm) than in the case of application of commercial  $\text{Si}_3\text{N}_4$  powder.

If commercial powders are applied, the formation of  $\alpha$ -SiAlON takes place directly from  $\alpha$ - $\text{Si}_3\text{N}_4$ , but for nanopowders the  $\beta$ -SiAlON forms first of all, which transforms to the  $\alpha$ -SiAlON at higher temperatures.

The hardness of obtained materials is directly related to their density and for samples prepared from nanopowders by sintering at 1650 °C was in a range of  $\text{HV}_5 = 18\text{--}23$  GPa. Fracture toughness grows with the rising sintering temperature and growth of needle-like grains and reaches  $6 \text{ MPa m}^{1/2}$  for samples sintered at 1650 °C.

## Acknowledgement

This work is funded within contract TST5-CT-2006-031462 of the 6FP program of the European Community.

## References

1. Zhilinska, N., Zalite, I., Krumina, A., Costin, W. and Mozdzen, G., Sintern der Materialien auf der Basis unterschiedlicher  $\text{Si}_3\text{N}_4$ -Pulver. *Verbundwerkstoffe*, 14. In *Symposium Verbundwerkstoffe*, herausgegeben von H.P.Degischer, 2003, pp. 399–404.
2. Herrmann, M., Schulz, I. and Zalite, I., Materials based on nanosized  $\beta$ - $\text{Si}_3\text{N}_4$  composite powders. *J. Eur. Ceram. Soc.*, 2004, **24**(12), 3327–3335.
3. Schulz, I., Herrmann, M. and Zalite, I., Development of nano- $\text{Si}_3\text{N}_4$ -materials and their applications. In *First Vienna international conference micro- and nano-technology*, 2005, ISBN 3-901657-18-5, pp. 1–10.
4. Zalite, I. and Grabis, J., Nanosize powders of refractory compounds for obtaining of fine-grained ceramic materials. *Mater. Sci. Forum*, 2007, **555**, 267–272.
5. Kurama, S., Herrmann, M. and Mandal, H., The effect of processing conditions, amount of additives and composition on the microstructure and mechanical properties of  $\alpha$ -SiAlON ceramics. *J. Eur. Ceram. Soc.*, 2002, **22**(1), 109–119.
6. Bulic, F., Zalite, I. and Zhilinska, I. N., Comparison of plasma-chemical synthesised SiAlON nano-powder and conventional prepared SiAlON powder. *J. Eur. Ceram. Soc.*, 2004, **24**, 3303–3306.